The SAS Gamma-Ray Spectrometer

Edison Liang, Andriy Dashko, Kelly Yao, Willie Lo, Hannah Hasson, Aileen Zhang, Rice University, Houston TX 77005; Gary Wong, Yuxuan Zhang, MD Anderson Cancer Center, Houston, TX 77005; Hernan Quevedo, Todd Ditmire, UT Austin, TX 78712.

Abstract

A new type of compact high-resolution high-sensitivity gamma-ray spectrometer for short-pulse gamma-rays has been developed by combining the principles of scintillators and attenuation spectrometers. The first prototype of this scintillator attenuation spectrometer (SAS) was tested successfully in 2015 on Trident laser experiments and later versions have since been used extensively in TPW laser experiments in Austin TX and in OMEGA-EP laser experiments at LLE, Rochester, NY. Here we give a concise description of the design principles, capabilities and preliminary results of the SAS.

1. Introduction

Conventional gamma-ray spectrometers use the "single photon counting" method by employing scintillators (NaI, CsI, BGO etc) coupled to photo-multiplier tubes (PMT), or cryogenic solid-state (e.g. Ge) detectors. Each gamma-ray deposits all of its energy in the scintillator or solid-state detector, converting its energy into optical photons, photoelectrons, which are then amplified for electron current readout. The gamma-ray spectrum is built up one photon at a time by measuring the total energy deposited by each gamma-ray. In this approach consecutive gamma-rays arriving at the detector must be separated in time longer than the scintillation plus electronic readout time, typically > ns Otherwise multiple gamma-rays cannot be distinguished from a single high energy gamma-ray. Hence single-photon-counting gamma-ray spectrometers cannot be used in short-pulse intense laser experiments, where a large number of gamma-rays are emitted in ps to sub-ps time scales, much shorter than the scintillation plus PMT readout time.

Conventional filter-stack attenuation spectrometer (FSS), made up of a series of high-Z filters arranged in tandem (Chen C.D. et al 2009) or configured as step wedges, has been the main diagnostic to measure continuum gamma-ray spectrum in laser experiments. However, FSS allows only a small number of energy channels (typically < 20) and works only up to a few MeV. For gamma-rays with energy ≥ 4-5 MeV, the mass attenuation coefficient reverses its decline and rises with increasing energy due to pair production (Heitler 1954). At these energies the attenuation length can no longer provide an unambiguous measure of the gamma-ray energy, even though detailed Monte Carlo simulations can provide some constraints on the spectral shape up to ~ 10 MeV. Other techniques that have been tried to measure short-pulse laser-created gamma-ray energies include nuclear activation thresholds (Leemans et al. 2001) and Forward Compton scattering (FCS, Morgan et al. 1991, Kojima et al 2014). None of these techniques can provide high-resolution high-sensitivity spectrometry for short-pulse laser-created gamma-rays.

Over the past several years, a collaboration between Rice University and the medical imaging group at the MD Anderson Cancer Center in Houston, has developed a new type of gamma-ray spectrometer, which we will call scintillation attenuation spectrometer (SAS). The idea is to image the 2-dimensional (2-D) scintillation light pattern emitted from

a finely pixelated (with mm-sized pixels) scintillator matrix block when it is irradiated by a narrow collimated beam of gamma-rays. Since the energy deposition pattern in the scintillator block varies with incident gamma-ray energy, such 2-D scintillation light profiles can in principle be used to reconstruct the incident gamma-ray spectrum, provided the emerging scintillation light profile faithfully reproduce the local energy deposition pattern of the gamma-rays. For this technique to work well, we need to (a) make each pixel 100% internally reflective except at the front surface, so that the energy deposited in each pixel is fully converted into scintillation light emerging only from the front surface of that pixel, (b) use the smallest crystal pixel that is practical to maximize the spatial resolution and minimize the internal absorption of the optical light, (c) use scintillation material with the highest light output for each MeV of absorbed gamma-ray energy, (d) use the highest-Z and highest-density scintillator material that attenuate gamma-rays most efficiently. Guided by these four principles and optimization among the many conflicting requirements, we created a working prototype of the SAS after many trials and errors, using mm-sized ce-doped LYSO scintillator crystals manually coated with a special low-Z ultra-thin reflector optimized for 420 nm photons. The cutting, polishing and coating process is highly labor intensive and requires many specialized equipments. Ce-doped LYSO was the preferred scintillator because of its high-Z, high-density (7.8 gm/cc) and high light output (50000 blue photons per MeV absorbed). The first SAS prototype, consisting of a 24 x 36 matrix of 1.5mm x1.5mm x 10mm pixelated LYSO crystals was successfully demonstrated in the summer of 2015 in a Trident laser experiment at LANL. Despite the low quality of the image (Fig1) due to the crude CCD camera used and light leakage from the container box, the proof-of-principle experiment demonstrated the utility and functionality of the SAS in short-pulse laser experiments. This ground breaking experiment at Trident demonstrated several important results which provide confidence in the successful construction of a high-resolution compact SAS for laser, fusion and many other ultra-intense gamma-ray applications. (a) The LYSO crystals produced abundant light that can be easily imaged using standard CCD cameras without intensification or cryogenics. (b) The gamma-rays lit up all 36 longitudinal pixels. This means we can enlarge the crystal block to include many more pixels, and still have measurable light from all pixels. (c) The 2-D light output patterns produced by different incident gamma ray energies are clearly distinguishable. (d) The intense EMP and neutron flux were not detrimental to the SAS performance.
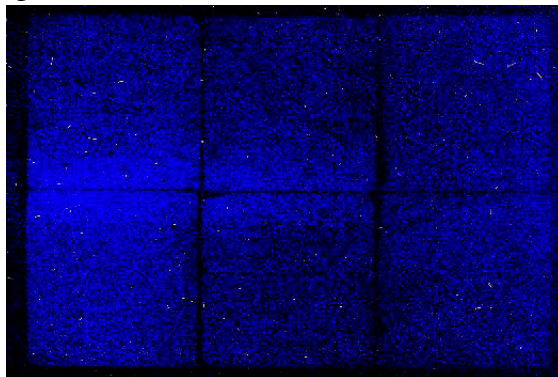

Fig.1 Scintillation light image of an early SAS prototype (24 x 36 pixels) for gamma-rays emitted by a high-Z target in a 2015 Trident laser experiment. The SAS was located at 1 meter from the laser target in this shot.

We emphasize that pixelated scintillator blocks of NaI and CsI have been used in past high energy physics experiments, and also in some recent LWFA laser experiments (Belm et al 2018). However, these detectors were designed for gamma-rays with energies in the 10 MeV to ≥ GeV range. Because high energy gamma-rays require large scintillation depths, especially in NaI and CsI, large scintillator blocks must be used, resulting in a large (~meter-sized) detector, low light intensity and low spectral resolution. In most cases only crude model input spectra with a few parameters can be meaningfully constrained via iterative Monte Carlo simulations to match the observed light profiles (Belm et al 2018). To our knowledge none of the previous pixelated scintillator spectrometers were designed to provide the full reconstruction of completely unknown input spectrum with high spectral resolution, which is the goal of the SAS.

2. SAS Design and Sample Results

After the successful proof-of-principle demonstration at the Trident laser in 2015, we constructed full-scale 36x48 LYSO matrix blocks (Fig.2) and used them in our TPW experiments of 2016 and 2018. Currently our largest LYSO matrix block measures 36 x 60, which can fully capture the scintillation light output of gamma-rays up to 50 MeV. We have upgraded the CCD camera to a sensitive high-speed non-cryogenic camera with wide-field lens and a CCD chip optimized for 420 nm light, plus remote control and data-link. The SAS apparatus is housed in a light-tight box approximately the size of a shoe box (Fig.3), with thick lead shielding all around and a 3 mm - 6 mm pinhole for the collimation of incident gamma-rays. The crystal holder can be easily adapted to accommodate matrix blocks of different sizes.
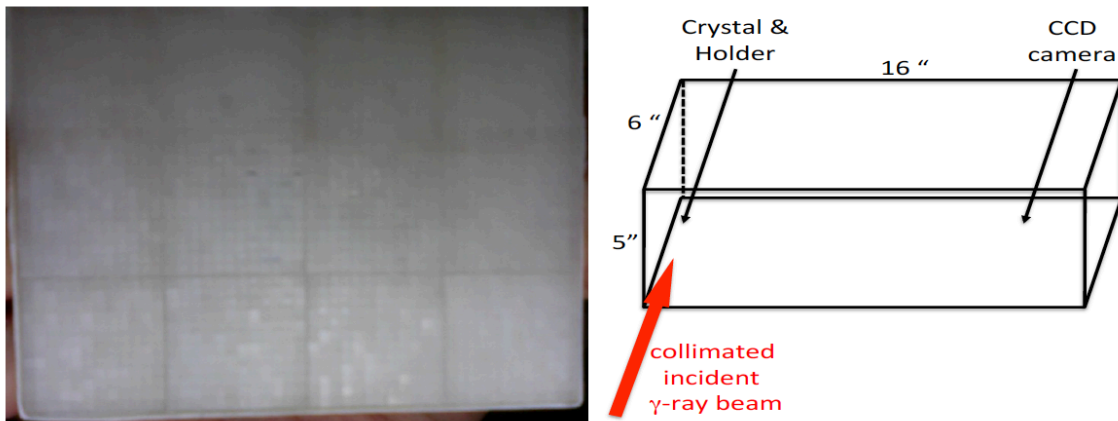

Fig.2 (above left) Image of the pixelated scintillator matrix block in the SAS used in the 2016 TPW experiments consisting of 36 x 48 1.5mmx1.5mmx10mm LYSO pixels. The entire block measures 6 cm H x 8 cm W x 1 cm D. Collimated gamma-rays enter the crystal block from the center of the left edge.

Fig.3 (above right) Sketch of the SAS layout with overall dimensions. Not shown are the external and internal lead shields with 3mm – 6mm pinholes used to collimate the incident gamma-ray beam. The lens of the CCD camera is positioned at ~18 cm from the scintillator block to provide the best image.

Fig.4 shows a typical SAS raw image taken during the 2016 TPW experimental run using 6mm pinhole collimators, while Fig.5 shows the corresponding GEANT4 simulated light pattern. Fig.6 shows GEANT4-simulated SAS images of various monoenergetic incident gamma-rays to highlight the gradual change of light pattern with gamma-ray energy. The transition from the "candle light" pattern (left) of 0.5 MeV gamma-rays to the "tear drop" pattern (right) of 50 MeV gamma-rays is caused by the domination of photoelectric effect in the former case, and pair production in the latter case. Compton electrons dominate in the middle panel for 5 MeV gamma-rays. For 50 MeV gammas-rays, it takes up to 60 longitudinal pixels to fully capture their light output. Fig.7 shows SAS images at two different detector angles from our 2018 TPW experiment using 3mm pinhole collimators. It demonstrates that the gamma-rays emitted at the target normal direction is much harder than those emitted at 90º from target normal. Starting in 2020 one of our SAS units was deployed at OMEGA-EP to measure the gamma-rays from short-pulse experiments. Preliminary results show that the SAS provides high-quality signals for OMEGA-EP shots.

comparison of SAS image with sample GEANT4
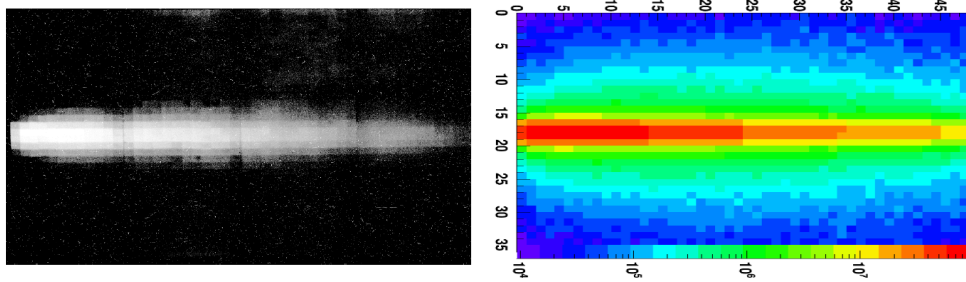simulation of ~10 MeV bremsstrahlung shows reasonable agreement

Fig.4 (left) SAS CCD raw image of LYSO scintillation light from a typical 2016 TPW shot. Gamma-rays entered from a 6mm diameter pinhole on the left. This image shows over 400 bright pixels, which in principle can be deconvolved into a gamma-ray spectrum of up to 200 energy channels.

Fig.5 (right) GEANT4-simulated SAS image of a 10 MeV bremsstrahlung input spectrum, showing strong resemblance to the SAS image in Fig.4. Subsequent deconvolution using the full 200x200 DRM gives the best-fit bremsstrahlung temperature of ~11+/-1MeV (see Fig.10).

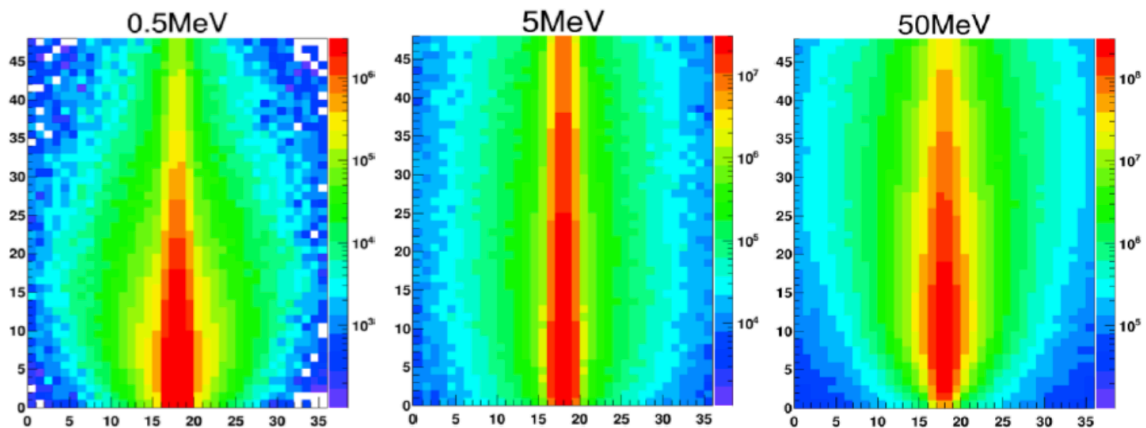light patterns from different monoenergetic gamma-rays are clearly distinguishable

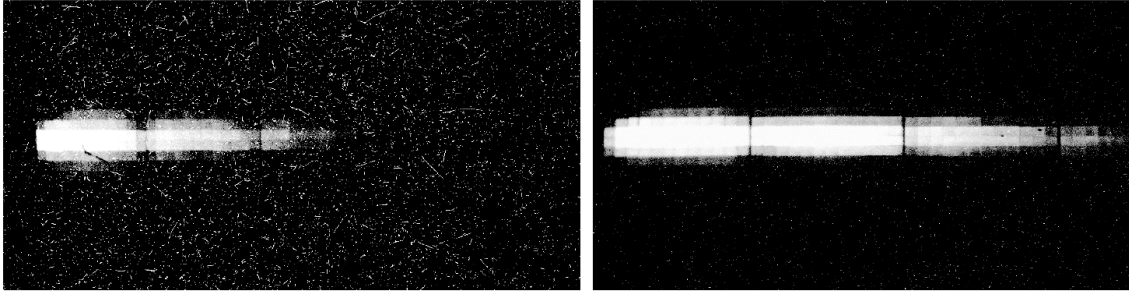**Fig.6** GEANT4-simulated scintillation light patterns for different monoenergetic gamma-ray energies.

Fig.7 Two SAS raw images from a 2018 TPW shot using 3 mm pinholes. The left image comes from an SAS located at ~ 90º from target normal. The right image comes from another SAS located at target normal. These images clearly demonstrate that the gamma-rays emitted at target normal are much harder than those emitted at ~ 90º. The CCD used to obtain the left picture is 50% more sensitive than the CCD used to obtain the right picture. Hence the background is higher even though the signal is weaker.
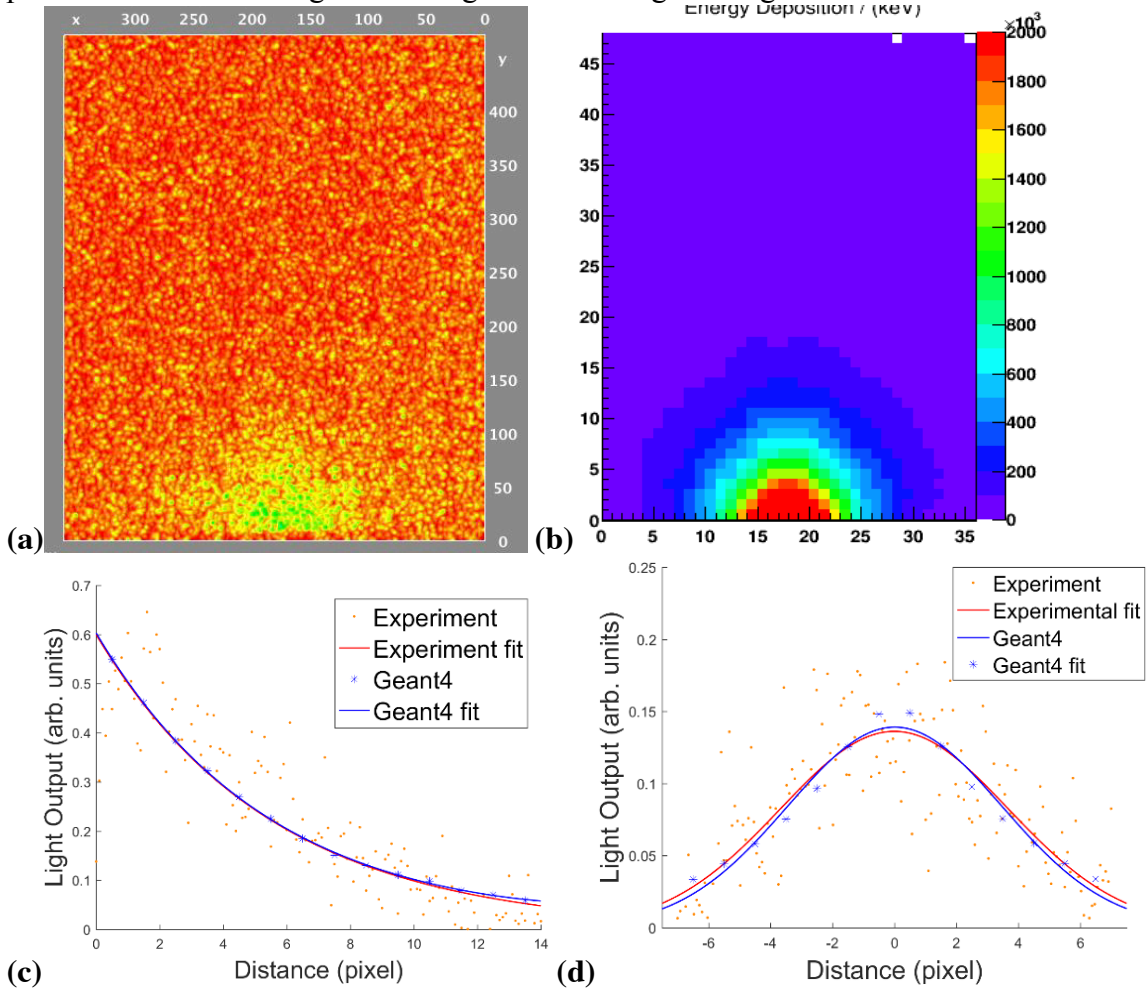

Fig.8 Calibration of the SAS using a ^{137}Cs source. (a) is raw SAS image, (b) is GEANT4 simulated image, (c) is the SAS longitudinal light profile compared to the corresponding GEANT4 simulated profile, (d) is the SAS transverse light profile compared to the

5

corresponding GEANT4 simulated profile. The agreements between experimental data and GEANT4 predictions are excellent. This validates the GEANT4 results.

We have carefully calibrated the SAS in the laboratory using gamma-ray emitting isotopes such as ^{137}Cs, ^{22}Na and ^{207}Bi. Fig.8 shows the results for ^{137}Cs (0.67 MeV). We see that the SAS data agrees well with GEANT4 predictions, which gives us confidence in the validity of the GEANT4 simulations of the SAS response.

3. Deconvolution of Gamma-Ray Spectrum from raw SAS Image

As for all gamma-ray spectrometers, the first step to reconstruct the incident spectrum from the detector signal is to build up a detector response matrix (DRM) using Monte Carlo simulations, which maps the incident gamma-ray energies to the light output from each pixel. We have completed 200 GEANT4 simulations, by injecting monoenergetic gamma-rays from 0.25 MeV to 50 MeV at 0.25 MeV intervals, using 10^6 particles per run. This allows us to construct a 200x200 DRM, which maps 200 gamma-ray energy channels onto the scintillation light output of 200 SAS pixels (Fig.9). We used a sophisticated and detailed computer model of the 36 x 48 LYSO matrix, including not only the elemental composition and geometry of each LYSO pixel, but also the low-Z reflectors and glue between the pixels used to form the matrix, since they may affect the secondary electron (and positron) transport. We have used this DRM to perform trial deconvolution of the incident gamma-ray spectra from our stockpile of SAS data, employing a variety of advanced inversion algorithms. This labor intensive work is ongoing. Fig.10 and Fig.11 showcase two such model spectra based on the raw images of Fig.4 and Fig.8 respectively. In both cases we started with a polynomial model trial spectrum. Fig.10 (a) shows a best-fit exponential spectrum with kT$_\gamma$ ~ 11 +/- 1 MeV with low-energy turnover at ~ 5 MeV. Fig.10 (b) shows that the spectral slope above the peak appears robust using different regularization techniques. Fig.11 shows a 2-component best-fit spectrum with the soft component dominating below ~ 2.5 MeV and the hard component dominating above ~ 5 MeV.
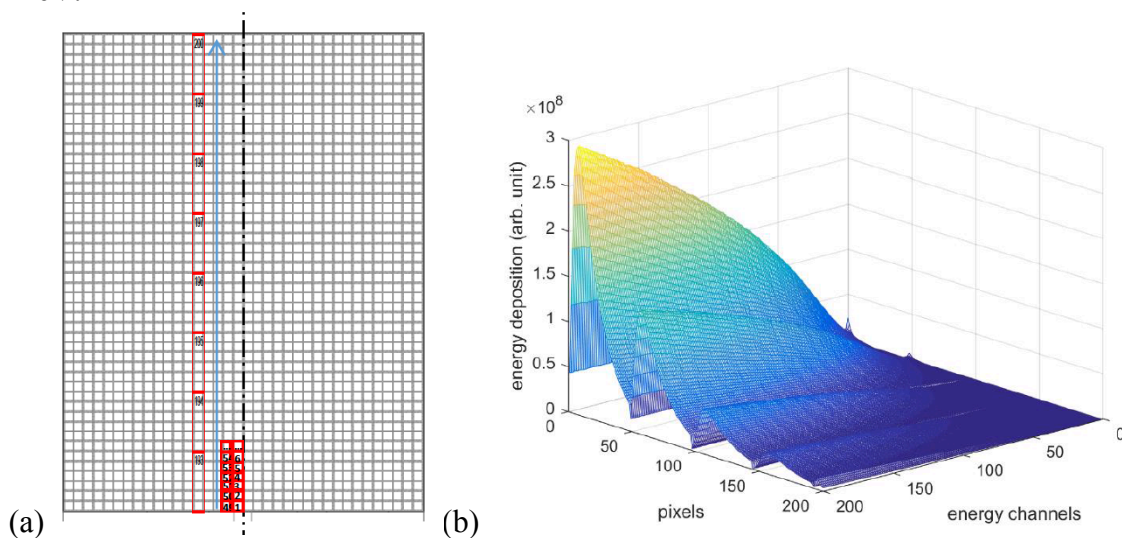

(a) (b)

Fig.9 (a) Labeling of the pixel number starting from the center line of the 36 x 48 LYSO matrix: pixels 1 – 48 denote first column, pixels 49-96 denote second column etc. However in the fifth column we combine 5 LYSO pixels into 1 pixel due to the faintness of the light

output. Gamma-rays enter the matrix from the bottom center. Left and right halves of the matrix are assumed to be reflection symmetric, so that their light outputs are averaged to compute the DRM. (**b**) 200 x 200 DRM obtained by 200 GEANT4 simulations in a 3D contour plot, for a 36 x 48 LYSO matrix and 6 mm pinhole. We assume that the scintillation light output of each LYSO pixel is proportional to the total energy deposited inside that pixel. The folded accordion pattern of the DRM is due to the way we order the pixel number in Figure (a).
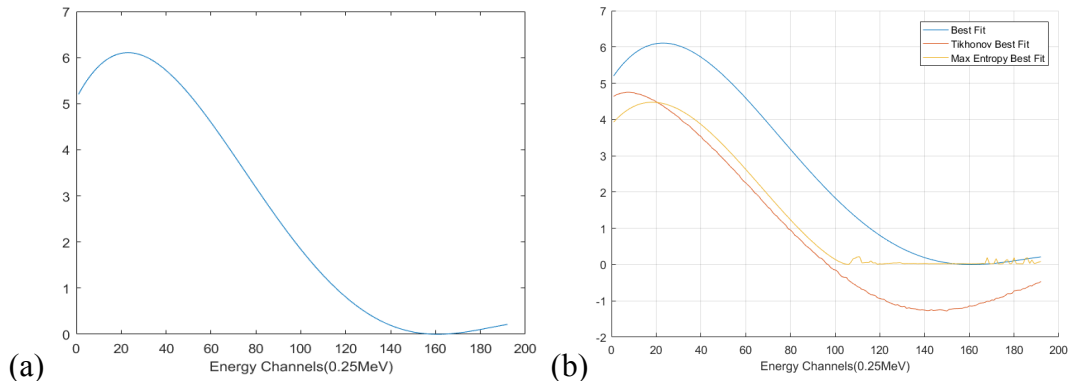

(a)   (b)

Fig.10 (a) Best-fit gamma-ray spectrum derived from the SAS image of Fig.4. The slope of this spectrum above the peak is consistent with a bremsstrahlung temperature of 11+/- 1 MeV. **(b)** Gamma-ray spectra (not normalized) deconvolved using three different techniques from the SAS image of Fig.4. Even though the three spectra peak at slightly different energies, they have identical slopes above the peak. Hence we are confident that the predicted bremsstrahlung temperature of 11 +/- 1 MeV is robust. The vertical scales are not normalized among the different model spectra.

Because the 200x200 detector response matrix **D** is semi-degenerate or almost-singular, direct inversion techniques are impractical. Hence we have focused on techniques based on forward folding via regularization of the matrix equation $\mathbf{Dx} - \mathbf{y} = 0$, where **x** is the input gamma-ray spectrum and **y** is the SAS image. Regularization methods that we have explored include the Tikhonov method, modified truncated SVD, damped truncated SVD, Ridge regression (also called Tikhonov regularization), Lasso regression, particle swarm and many other techniques. Among them, Ridge and Lasso regressions are representative of most other methods which are variations or combinations of Ridge and Lasso methods. Lasso regression is an iterative process that finally converges the result to a certain value. Ridge regression stabilizes the solution by presuming that the spectrum is smooth and then introducing an error factor λ into the least-square minimization problem $\|\mathbf{Dx}-\mathbf{y}\|^2$. The problem is reduced to minimizing $\|\mathbf{Dx}-\mathbf{y}\|^2+\lambda^2\|\mathbf{x}\|^2$. Since the full DRM is extremely ill-conditioned, in most cases only if we allow a huge error factor λ, which is comparable to the actual data itself, can the random noise be completely reduced and the underlying pattern be shown. In general, Ridge is more suitable for deconvolving a continuum input spectrum and Lasso is more suitable for deconvolving narrow lines. In tests, we find that for a monoenergetic input spectrum, Lasso is able to reproduce the peak energy with little error, while Ridge forms a broad continuum with the highest point located at the peak of the input spectrum. On the other hand, Ridge gives better results when the
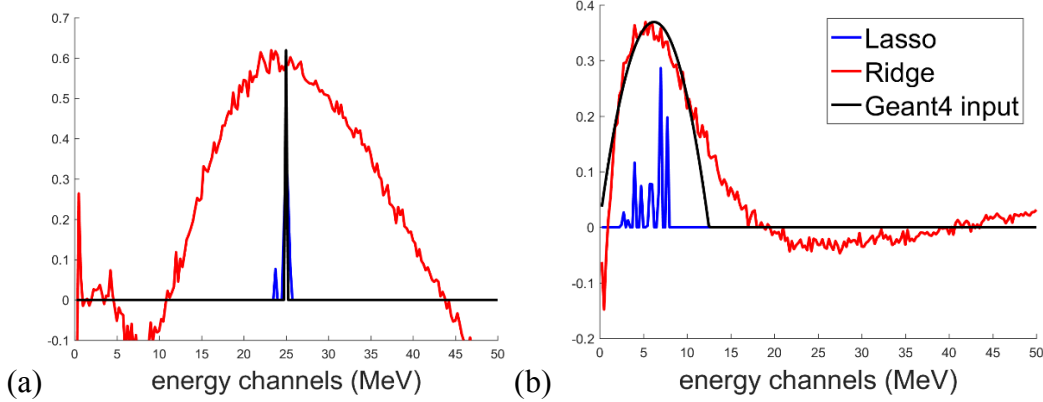
Fig.11 (a) A narrow 25 MeV gamma-ray line is injected into the LYSO matrix and its GEANT4 output is deconvolved using the Lasso and Ridge regressions. Here Lasso gives much better results than Ridge. **(b)** A broad gamma-ray "bump" centered at 6 MeV is injected into the LYSO matrix and its GEANT4 output is deconvolved using the Lasso and Ridge regressions. Here Ridge gives much better results than Lasso.

input spectrum is a smooth broad continuum. Fig.11 illustrates the advantages and disadvantages of using the Lasso vs. Ridge regressions for different input spectral shapes.

One of the problems of regularizing the full 200 x 200 DRM is that the matrix dimension is too big. By decreasing the dimension number from 200 to, for example, 48, the condition number of the DRM is lowered, which leads to a smaller error factor λ for Ridge regression and more stable solution. The most natural way to reduce the pixel number from 200 to 48, is to simply collapse the transverse dimension of the matrix by combining the light output of all horizontal pixels in Fig.9(a), so that only the total light distribution along the 48 longitudinal pixels is used in the deconvolution. For example the continuum spectra of Fig.10 and Fig.11 are obtained using variations of the Ridge regression method based on the reduced 48 x 48 longitudinal DRM (LDRM). However, we emphasize that by collapsing the full 200 pixels into only 48 longitudinal pixels, we are throwing out valuable information on the transverse light distribution: the variation of the transverse light distribution with gamma-ray energy (Fig.6) is now lost. We have been searching for a compromise solution by including a few additional "transverse pixels" which maximally captures the variation of the transverse light distribution with gamma-ray energy. This work is in progress.
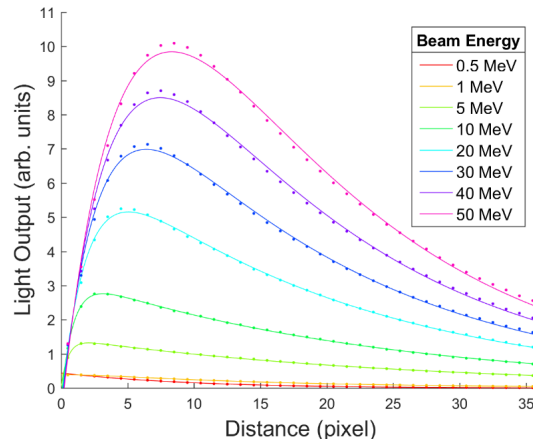
Fig.12 Light outputs in the longitudinal direction as a function of pixel number (for incident gamma-ray beam of 6.0 mm diameter, averaged among 8 transverse pixels).

As it turns out for the 48 x 48 LDMR, there is an alternative, semi-analytic method to deconvolve an incident gamma-ray spectrum from the longitudinal light distribution. Fig.12 is a plot of the transverse-averaged light profiles as functions of the longitudinal pixel number x for a sample of monoenergetic incident gamma-ray energies. These curves can be well fit with a double exponential function $f(x) = a\, e^{-bx} + c\, e^{-dx}$, where the constants (a, b, c, d) are in turn well fit by analytic functions of E for E > 1 MeV. As a result, the longitudinal light profile f(x) for any input gamma-ray spectrum g(E) can be written as an integral equation for g(E) (Tricomi 1957):

$$f(x) = \int dE\, g(E)\, \{a(E)\, \exp(-b(E)\, x) + c(E)\, \exp(-d(E)\, x)\}.$$

For a given f(x), g(E) can in principle be solved using various iteration or variational methods (Phillips 1962, Hansen 1992, Hansen 2007, Yagle 2005). In the special cases when g(E) can be modeled analytically as a polynomial or sum of exponential functions, the integral over dE of each term can be evaluated analytically as Laplace transforms, and the solution for g(E) can be obtained by R^2-minimization of the expansion coefficients. This semi-analytic approach, though approximate, is much faster than regularizing the full 48 x 48 matrix. In any case this method can be used to independently cross check the matrix regularization results.

4. Discussion and Summary

In this paper we have presented the basic design and some preliminary results of a new type of gamma-ray spectrometer called the SAS, which combines the physics principles of attenuation and scintillation. The key innovation is the use of mm-scale pixelated LYSO crystals with 100% reflective coating to form a large matrix that can fully capture gamma-rays up to 50 MeV in a compact volume. The abundant light output of LYSO crystals provides high signal-to-noise even at low gamma-ray fluence, and the high speed CCD camera allows millisecond exposures, ideal for high-rep rate laser applications. Much work remains to be done on the spectral deconvolution algorithms since the detector response matrix is semi-degenerate, requiring advance numerical schemes to achieve a stable robust spectrum.

References

Behm, K.T. et al 2018, Rev. Sci. Instr. 89, 113303.

Chen, C.D. et al. 2009, Phys. Of Plasmas, 16, 082705.

Hansen, C., 2007, Num. Algo. 46 189; also available as regtools.Mathworks, 16 Apr 1998 (Updated 01 Feb 2015), www.mathworks.com/matlabcentral/fileexchange/52-regtools.

Hansen, P.C. 1992, Inverse Problems 8, 849.

Heitler, W. 1954, *Quantum Theory of Radiation* (Oxford, UK).

Kojima, S. et al 2014, Plasma and Fusion Res. 9, 4405109.

Leemans, W. et al. 2001, Phys. Of Plasmas 8, 2510.

Morgan, G. et al. 1991, Nucl. Inst. & Meth. in Phys. Res. A 3080 544.

Phillips, B.I. 1962, J. Ass. Comp. Mach. 9, 84.

Tricomi, F.G. 1957, *Integral Equations* (Interscience, NY).

Yagle, A. E. 2005 *Regularized Matrix Computations,* available at web.eecs.umich.edu/~aey/recent/regular.pdf